Academic Journal of Science and Technology
ISSN: 2771-3032 | Vol. 10, No. 1, 2024

First-principles Calculations of The Elastic Properties, Electronic Structure and Optical Properties of Hexagonal Al_4SiC_4

Zongye Li*, Ailiang Yin

School of Electronic Information, Southwest Minzu University, Chengdu, China
*Corresponding author: ZongYe Li

Abstract: The crystal structure, elastic constants, electronic structure and optical properties of Al_4SiC_4 Have been systematically investigated using the first principles calculation method based on density functional theory. The calculated lattice constants and elastic constants are consistent with the experimental and calculated values, and it shows that the hexagonal Al_4SiC_4 crystal structure is stable. The calculated bulk, shear, Young's modulus and Poisson's ratio of hexagonal Al_4SiC_4 are in accordance with the values in the literature. The calculated band gap of the Al_4SiC_4 is 1.076 eV. The changes of optical response functions of hexagonal Al_4SiC_4 in the (100) and (001) directions with photon energy are calculated, including complex dielectric function, complex refractive in-dex, absorption spectrum and reflection spectrum. In the (100) and (001) directions, the static dielectric con-stants are 7.74 and 8.96,respectively,and the refractive indexes are 2.78 and 2.99,respectively. The calcu-lated results can provide theoretical basis for related applications.

Keywords: Al_4SiC_4; Electronic structure; Optical properties; First-principles.

1. Introduction

Al_4SiC_4 ceramic is characterized by its low density (3.03 g /cm3), high melting point (> 2700℃), high chemical stability, high strength, low thermal expansion coefficient and excellent oxidation and hydration resistance. It has become a promising high-temperature structural material and high-performance refractory material to be developed, and has gradually attracted people's attention in the fields of aerospace structural ceramics and high-temperature electronic semiconductors [1][6].Since Barczak et al.[7] first discovered Al_4SiC_4, several research groups [2][5][8][10] have focused on the synthesis and preparation of Al_4SiC_4 (such as solid-state reaction sintering method, chemical vapor deposition).Experimental study on the properties and applications of volume-solid phase sintering method, hot pressing sintering method, high temperature self-spreading method, penetration method, mechanical alloying method, etc.[3][11][20] .Inoue et al. [1] used a mixture of aluminum, silicon and carbon and a mixture of kaolin, aluminum and carbon as raw materials to synthesize Al_4SiC_4 powder by two-step method, and then conducted pulse current sintering to synthesize massive Al_4SiC_4. Yamamoto et al. [2] prepared Al_4SiC_4 powder with aluminum, silicon and carbon black as raw materials. Huang et al. [3] studied the high temperature oxidation resistance and high temperature mechanical properties of Al_4SiC_4 prepared by reactive hot pressing sintering, and obtained that the bending strength increased with the increase of temperature within the test temperature range of 1000 ~ 1300℃.Wen et Al [4] used Al, graphite powder and polycarbosilane (PCS) as raw materials to prepare Al_4SiC_4 bulk ceramics by reactive hot pressing method, and studied the mechanical properties, thermal properties and oxidation behavior of Al_4SiC_4 ceramics.Solozhenko et al. [14] synthesized Al_4SiC_4 polycrystalline samples by reacting aluminum with graphite and silicon, and fitted the experimental data of pressure and volume (p-V) with Birch equation of state to obtain a volume modulus of 180.2 GPa.In recent years, theoretical studies on Al_4SiC_4 have also been reported, but not many [21][27], mainly focusing on the calculation of material properties based on first principles, such as lattice constants, elastic properties, band structure, optical properties and thermodynamic properties[21],[22],[24],[28] .Li et al. [24] calculated the phonon spectrum, chemical bond, thermal and thermodynamic properties of Al_4SiC_4 using density functional theory, and obtained that the linear thermal expansion coefficient of Al_4SiC_4 in the direction [001] was slightly higher In the direction [100].Liao et al. [25] have studied the bonding properties, elastic stiffness and ideal strength of Al_4SiC_4, and the results show that the mechanical properties of Al_4SiC_4 are closely related to the crystal structure, and the volume modulus is 179 GPa, the shear modulus is 140 GPa, and the lattice parameter is a = 3.222 A. c = 21.352 A.So far, there are few theoretical studies on the elastic properties, electronic structure and optical properties of Al_4SiC_4 including complex dielectric function, complex refractive index, absorption spectrum and reflection spectrum.Therefore, in this paper, the elastic properties, electronic structure and optical properties of Al_4SiC_4 are calculated using the mode conservation pseudopotential based on density functional theory, and the relationship between them is analyzed theoretically, which provides a theoretical basis for the practical application of Al_4SiC_4.

2. Computational Methods

This paper adopts the first principles calculation method based on density functional theory, and all the calculations are completed on the Cambridge Sequential To tal Energy Package(CASTEP)[29] module.In the calculation process, Perdew-Burke-Ernzerhof (PBE) method on Gener-al gradient approximation (GGA) is selected for exchange correlation terms[30] . The interaction potential between ions and valence electrons is described by the mode conservation

pseudopotential.The valence electrons involved in the calculation are Al: $3s^2 3p^1$, Si: $3s^2 3p^2$, C: $2s^2 2p^2$.The Broyden-Fletcher-Goldfarb-Shanno (BFGS) algorithm was used to optimize the structure of the cell model, and the truncation energy was set to 750 eV. The self-consistent cyclic convergence accuracy is 5.0×10^{-7}eV/atom, the stress error between atoms is less than 0.02 GPa, the maximum displacement convergence error between atoms is less than 5.0×10^{-4}A, and the total energy convergence standard of the system is 5.0×10^{-6}eV/atom.The k point grid in Brillouin zone is 5 × 5 × 2.

3. Result and Discussion

3.1. Lattice parameter

Al_4SiC_4 is a hexagonal system with space group P63mc [11], group number 186, lattice constant a = b = 3.2771 Å, c = 21.676 Å, V = 201.60 Å, α = β = 90°, γ = 120°.The crystal structure of Al4SiC4 is shown in Figure 1, where the purple is Al atom, the light gray is C atom, and the yellow is Si atom. Through the geometric structure optimization of Al_4SiC_4 cell, the lattice constant after optimization is obtained, as shown in Table 1. Compared with the experimental value [11], the difference between a and c is -0.63% and 0.31%, indicating that the model and calculation method adopted are credible.

Table 1. Calculated lattice parameters a, c (in Å) , and volume V (in $Å^3$) with the literature results for comparison

Method	*a*	*c*	*V*
Pres.	3. 2562	21. 6097	198. 427
Expt. [11]	3. 2771	21. 676	201. 60
Expt. [5]	3. 2812	21. 7042	—
Expt. [14]	3. 277	21. 74	201. 60
Calc. [25]	3. 222	21. 352	—
Calc. [22]	3. 282	21. 796	—

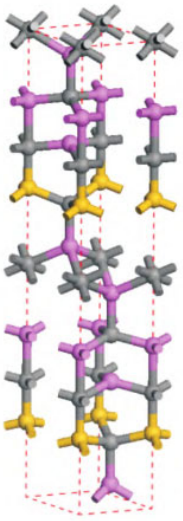

Figure 1. Crystal structures of Al_4SiC_4 . The purple, gray and yellow spheres represent the Al, C and Si ions, respectively.

3.2. Elastic property

For the hexagonal crystal phase Al_4SiC_4, there are five independent constants, respectively C_{11}, C_{12}, C_{13}, C_{33}, C_{44}, C_{66}= (C_{11}-C_{12}) /2, and the calculation results are shown in Table 2.As can be seen from Table 2, $C_{33} > C_{11} > C_{12} > C_{44} > C_{13} > 0$. According to the elastic stability criterion of hexagonal crystal structure [31] : C11-| C_{12}| > 0, $C_{44} > 0$, (C_{11}+ C_{12}) C_{33}-2 (C_{13})^2 > 0, it can be seen that the calculated elastic constant of Al_4SiC_4 satisfies the above stability conditions, so the crystal structure of Al_4SiC_4 is stable.

Table 2. Calculated secend order elastic constants (Cij in GPa) of Al_4SiC_4

Method	C_{11}	C_{12}	C_{13}	C_{33}	C_{44}	C_{66}
Pres.	389. 1	127. 9	46. 8	404. 4	110. 7	130. 6
Calc. [25]	386	118	50	409	122	134
Calc. [26]	369. 5	117	52. 9	383. 5	110. 2	121. 2

Based on the calculated elastic constant C_{ij}, the volume modulus and shear modulus can be obtained according to the Reuss-Voigt-Hill [32] model:

$$G_V = \frac{1}{15}(2C_{11} + C_{33} - C_{12} - 2C_{13}) + \frac{1}{5}(2C_{44} + \frac{C_{11} - C_{12}}{2})$$

$$G_R = 15\,[4(2S_{11} + S_{33}) - 4(S_{12} + 2S_{13}) + 6(S_{44} + S_{11} - S_{12})]^{-1}$$

$$B_V = \frac{1}{9}(2C_{11} + C_{33}) + \frac{2}{9}(C_{12} + 2C_{13})$$

$$B_R = [2S_{11} + S_{33}) + 2(S_{12} + 2S_{13})]^{-1}$$

$$G_H = (G_R + G_V)/2$$

$$B_H = (B_R + B_V)/2$$

Where S_{ij} is the elastic flexibility tensor, Poisson's ratio and Young's modulus can then be calculated:

$$\nu_X = \frac{3B_X - 2G_X}{2(3B_X + G_X)}$$

$$E_X = \frac{9G_X B_X}{3B_X + G_X}$$

Where X = Reuss, Voigt or Hill. The calculation results are shown in Table 3.The calculated bulk moduli of Reuss, Voigt and Hill are 186.0, 179.7, 18.2 GPa, respectively, which are consistent with the calculated values (179 GPa [25], 171.9 GPa [26]) and experimental value (182.0 GPA [14]) agree well, indicating that the calculation method is reasonable.The shear modulus is 134.5,129.3, 131.9 GPa, which is close to the value in the literature (140 GPa [25]).Bulk modulus B and shear modulus G represent the ability of materials to resist compressive deformation and shear strain, respectively. The ratio of shear modulus and bulk modulus G /B is widely used to characterize the ductility and brittleness of materials.According to an empirical criterion proposed by Pugh [33], when G /B > 0.57, the material is brittle, and when

G /B < 0.57, the material is ductile.In this paper, the G /B value of Al_4SiC_4 calculated by GGA-PBE method is 0.73, which is greater than the critical value of 0.57, indicating that Al_4SiC_4 is brittle, which is consistent with the predicted results of literature [26].

Table 3. Calculated bulk modulus BX(X = V, R, H) (in GPa) , shear modulus GX(in GPa) , Young's modulus EX(in GPa) , Poisson's Ratio νXwith the literature results for comparison

Method	B			G			E			ν_X		
	B_V	B_R	B_H	G_V	G_R	G_H	E_V	E_R	E_H	ν_V	ν_R	ν_H
Pres.	180. 6	179. 7	180. 2	134. 5	129. 3	131. 9	323. 2	312. 8	318. 0	0. 202	0. 210	0. 206
Calc.	172. 0 [26]	171. 7 [26]	179 [25] 171. 9 [26]	127. 0 [26]	123. 6 [26]	140 [25] 125. 3 [26]			302. 4 [26]			0. 206 [26]
Expt.		182. 0 [14]			—			—			—	

3.3. Electronic property

Band structure is an important basis for material analysis.The band structure of Al_4SiC_4 is shown in Figure 2.The dotted line in the figure represents the Fermi level. It can be seen from the figure that the conduction band base of Al_4SiC_4 is located at the high symmetric point M in the first Brillouin region, and the valence band top is located at the high symmetric point G in the first Brillouin region, so Al_4SiC_4 has an indirect band gap, which is consistent with the results reported by Forster et al. [21].The energy gap E_g = 1.076eV of Al_4SiC_4 is consistent with the calculated value (1.05eV [22], 1.12eV [26]), but lower than the experimental value (2-2.5eV[5]).Due to the deficiency of the calculation method in solving the excited state energy, the obtained band gap will be smaller than the experimental value, so the calculated value is smaller than the experimental value, but it does not affect the analysis of the band structure.

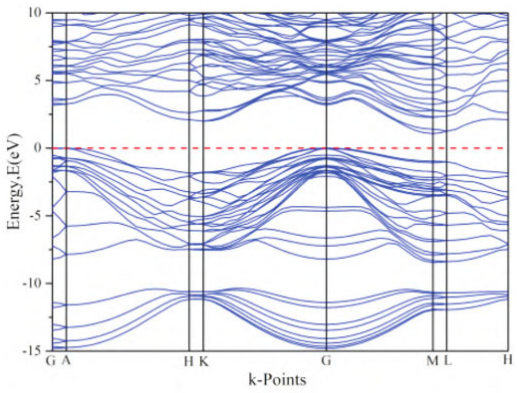

Figure 2. The band structure of Al_4SiC_4

Figure 3 shows the total state density and fractal density of Al_4SiC_4. As can be seen from Figure 3, it can be roughly divided into three regions: -15 eV ~ 10 eV, -8.8 eV ~ 0 eV, and 0 eV ~ 19.1 eV.In the low cost zone (-15 eV - 10 eV), it is mainly composed of Si-2s and C-2s electronic states, and the electron orbitals of the two atoms are hybridized, indicating that there is a strong covalent bond between the two atoms, so that the system has a more stable structure. The high valence zone (-8.8EV-0 eV) is mainly composed of SI-2P and C-2P electron states, and the density of states near the Fermi plane is mainly composed of p electron contributions of Al, Si and C atoms, and s electron contributions are less. The conduction band is mainly composed of Al-2p and Si-2p electron states.

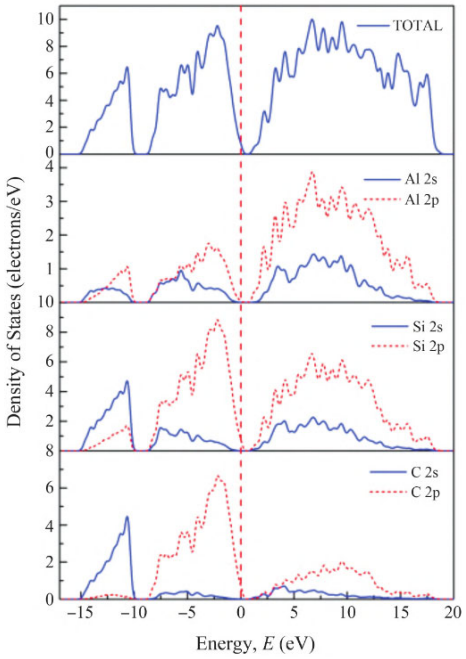

Figure 3. The total density of states and partial density of states of Al_4SiC_4

3.4. Optical property

3.4.1. Complex dielectric function

The macroscopic optical response of a solid can usually be described by the complex dielectric function $\varepsilon(\omega) = \varepsilon_1(\omega) + i\varepsilon_2(\omega)$, where ε1 and ε_2 are the real and imaginary parts of the complex dielectric function, respectively, and ω is the frequency of the photon.The calculated complex dielectric function curves of hexagonal crystal phase Al_4SiC_4 in the polarization direction of incident light along the a axis (100) and the c axis (001) are shown in Figure 4.

As can be seen from Figure 4, the static dielectric constant of Al_4SiC_4 in the direction of (100) and (001), that is, the value of zero frequency, is 7.74 and 8.96, respectively. In the direction of (100), in the low energy region, both the real and imaginary parts of the dielectric function increase with the increase of photon energy. The maximum value of the real part of the dielectric function at 4.38eV is 14, and the maximum value of the imaginary part at 5.86eV is 13.8, which is consistent with the results reported in the literature (the real part is 4.38eV [22], the imaginary part is 5.82eV [22]).Subsequently, the virtual part of the dielectric function decreases and approaches 0 after about 20 eV. The real part of the dielectric function decreases first and then rises, reaching the lowest value -4.12 at 9.07eV. The real part of the dielectric function increases slowly within the range of about 9 eV to

35 eV.In the direction of (001), the real part of the dielectric function reaches a maximum of 15.7 at 3.71 eV, and the imaginary part reaches a maximum of 15.3 at 5.32 eV.

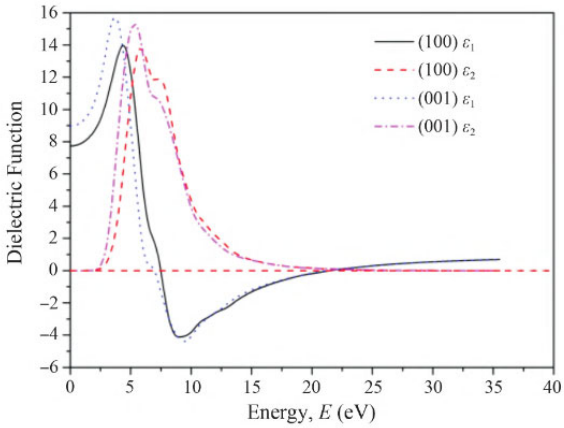

Figure 4. The complex dielectric functions of Al_4SiC_4

3.4.2. Complex refractive index

According to the relationship between dielectric function and complex refractive index: $\varepsilon_1 = n^2-k^2$, $\varepsilon_2 = 2nk$, (n is the refractive index, k is the extinction coefficient), the refractive index n and extinction coefficient k of the hexagonal crystal phase Al_4SiC_4 can be calculated along the polarization direction of the incident light along the a axis (100) and the c axis (001) with the photon energy. As shown in Figure 5.

As can be seen from Figure 5, the refractive index of Al4SiC4 at zero frequency in the direction of (100) and (001) is 2.78 and 2.99, respectively, which is consistent with the results reported in the literature (2.73 [22]).With the increase of photon energy, the refractive index first increases, then decreases and then increases.The refractive index along the direction (100) reaches a maximum value of 3.85 at 4.63 eV and a minimum value of 0.164 at 20.62 eV. The extinction coefficient starts to increase significantly at 2.02 eV, reaches a maximum value of 2.61 at 8.2 eV, and then decreases.The refractive index along the direction (001) reaches a maximum value of 4.06 at 3.94 eV and a minimum value of 0.159 at 19.58 eV.The extinction coefficient starts to increase significantly at 2.04 eV, reaches the first peak at 2.46 eV at 5.95 eV and then declines, then continues to rise to 8.43 eV, reaches the second peak at 2.50 eV, and then slowly decreases.

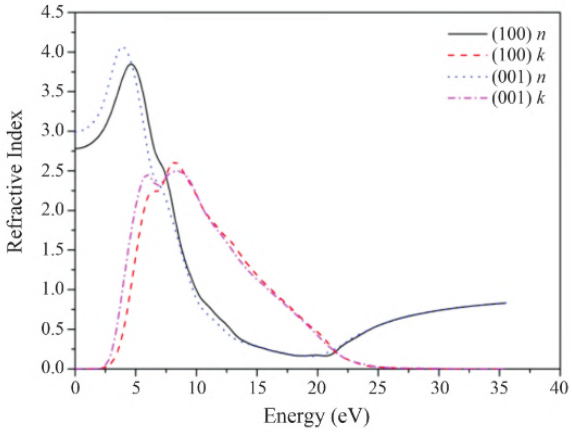

Figure 5. The complex refractive indexes of Al_4SiC_4

3.4.3. Absorption coefficient

Fig.6 shows the absorption coefficients of the hexagonal crystal phase Al_4SiC_4 along the polarization direction of the incident light along the a axis (100) and the c axis (001) with the photon energy.It can be seen that in the direction of (100) and (001), with the increase of photon energy, the absorption coefficient of Al_4SiC_4 first increases and then decreases, and the absorption coefficient is close to 0 after (0-2.5 eV) and 30 eV, respectively.The absorption coefficient reaches a peak value of 3.58×10^5/ cm at 8.98 eV in the direction of (100), and 3.62×10^5/ cm at 9.46 eV in the direction of (001).

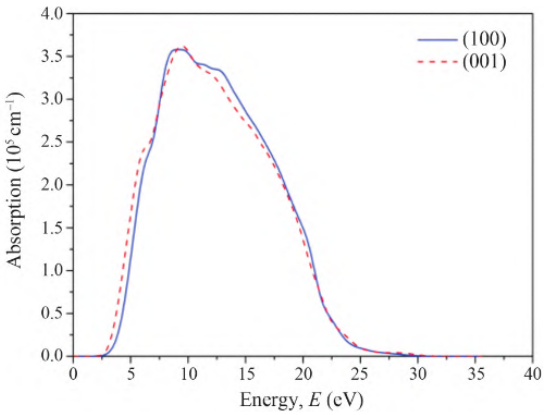

Figure 6. The absorption coefficients of Al_4SiC_4

3.4.4. Reflectance

Based on the relationship between reflectivity and rereflectivity [34]: $R(\omega) = \frac{(n-1)^2 + k^2}{(n+1)^2 + k^2}$,n is refractive index, k is extinction coefficient.The reflectance curve of Al_4SiC_4 along the a axis (100) and c axis (001) of the incident light polarization direction along with the photon energy can be obtained, and the calculation results are shown in Fig.7.As can be seen from Fig.7, the reflectance of Al_4SiC_4 in the direction of (100) and (001) generally increases with the increase of photon energy, at first shows a wave rise and then a rapid decline, and reaches a maximum value of 0.642 and 0.628 at 18.0 eV and 17.8 eV, respectively. When the photon energy is greater than 22 eV, the reflectance in both directions is almost the same.In the visible light energy range of 1.6eV ~ 3.2eV, the reflectance of (100) direction is between 24% ~ 29%, and the reflectance of (001) direction is between 27% ~ 35%, but the latter is slightly larger than the former. Materials with reflectance greater than 25% are generally considered to have a metallic luster.As a result, Al_4SiC_4 has a metallic luster.

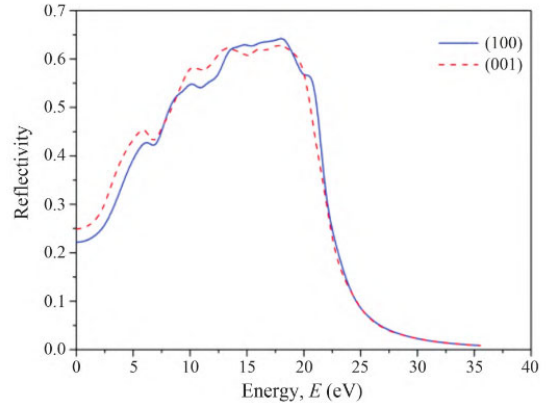

Figure 7. Thereflectivities of Al_4SiC_4

4. Conclusion

In this paper, the geometric structure parameters of the hexagonal crystal phase Al_4SiC_4 are optimized by using the generalized gradient approximate mode conservation pseudopotential method based on the framework of density functional theory. The elastic constant, band structure, state density, complex dielectric constant, complex refractive index, absorption coefficient and reflectivity of the hexagonal crystal phase Al_4SiC_4 are calculated and analyzed. It provides theoretical support for the practical application of hexagonal phase Al_4SiC_4.

References

[1] Inoue K, Yamaguchi A, Hashimoto S. Fabrication and oxidation resistance of Al4SiC4 body [J]. J. Ceram.Soc. Jpn., 2002, 110: 1010.

[2] Yamamoto O, Ohtani M, Sasamoto T. Preparation and oxidation of Al4SiC4[J]. J. Mater. Res., 2002, 17:774.

[3] Huang X X, Wen G W, Cheng X M. Oxidation resist-ance and mechanical properties of A14SiC4 ceramic at high temperature [J]. J. Mater. Eng., 2004 (12) : 32

[4] Wen G W, Huang X X. Increased high temperature strength and oxidation resistance of Al4SiC4 ceramics [J]. J. Eur. Ceram. Soc., 2006, 26: 1281.

[5] Zevgitis D, Chaix — Pluchery O, Doisneau B, et al.Synthesis and characterization of Al4SiC4: a “new”wide band gap semiconductor material [J]. Mater.Sci. Forum., 2015, 821: 974.

[6] Chen J H, Zhang Z H, Mi W J, et al. Fabrication and oxidation behavior of Al4SiC4 powders [J]. J. Am. Ce-ram. Soc., 2017, 100: 3145.

[7] Barczak V J. Optical and x — ray powder diffraction data for Al4SiC4 [J]. J. Am. Ceram. Soc., 1961, 44:299.

[8] Inoue K, Yamaguchi A. Synthesis of Al4SiC4 [J]. J.Am. Ceram.Soc., 2003, 86: 1028.

[9] Huang X X, Wen G W. Reaction synthesis of aluminum silicon carbide ceramics [J]. Mater. Chem. Phys., 2006, 97: 193.

[10] Lee J S, Lee S H, Nishimura T, et al. Synthesis of mono— phase, hexagonal plate — like Al4SiC4 powdervia a carbothermal reduction process [J]. J. Ceram.Soc.Jpn., 2008, 116: 717.

[11] Inoue Z, Inomata Y, Tanaka H, et al. X — ray crystallographic data on aluminum silicon carbide, α — Al4SiC4and Al4Si2C5 [J]. J. Mater. Sci., 1980, 15:575.

[12] Lee J S, Lee S H, Nishimura T, et al. Hexagonalplate — like ternary carbide particulates synthesized by a carbothermal reduction process: processing parameters and synthesis mechanism [J]. J. Am. Ceram. Soc., 2009, 92: 1030.

[13] Zhou W. Synthesis and properties of Al4SiC4 [D] Wu-han: Wuhan University of Science and Technology, 2010

[14] Solozhenko V L, Kurakevych O O. Equation of state of aluminum silicon carbide α — Al4SiC4 [J]. Solid StateCommun., 2005, 135: 87.

[15] Liu H, Zhang H H, Zhu M, et al. Pressureless sin-tered Al4SiC4ceramics with Y2O3 addition [J]. J.Eur. Ceram. Soc., 2023, 43: 4215.

[16] Liu J W, Zhou X B, Tatarko P, et al. Fabrication, microstructure, and properties of SiC/ Al4SiC4 multi-phase ceramics via an in — situ formed liquid phase sin-tering [J]. J. Adv. Ceram.2020, 9: 193.

[17] Nakashima Y, Kamiya R, Hyuga H, et al. Rapid fabrication of Al4SiC4 using a self — propagating high—temperature synthesis method [J]. Ceram. Int., 2020,46: 19228.

[18] Zhao C Y, Chen G Y, Guo C Y, et al. Preparation ofAl4SiC4 with higher aspect ratio by a novel two—step method [J]. Ceram. Int., 2022, 48: 23908.

[19] Yu C, Yuan W J, Deng C J, et al. Synthesis of hexagonal plate — like Al4SiC4 from calcined bauxite, silica and carbon black [J]. Powder Technol., 2013, 247:76.

[20] Xing G C, Deng C J, Ding J, et al. Fabrication and characterisation of Al N — Si C porous composite ceramics by nitridation of Al4SiC4 [J]. Ceram. Int., 2020, 46: 4959.

[21] Forster S, Chaussende D, Kalna K. Monte carlo simulations of electron transport characteristics of ternary carbide Al4SiC4 [J]. Appl. Energy Mater., 2019, 2:715.

[22] Hussain A, Aryal S, Rulis P, et al. Density functional calculations of the electronic structure and optical properties of the ternary carbides Al4Si C4and Al4Si2C5 [J]. Phys. Rev. B, 2008, 78: 195102.

[23] Li Y F, Xiao B, Sun L, et al. A theoretical study of dielectric tensor, Born effective charges, LO—TO splitting and infrared response of Al4SiC4 and Al4Si2C5 [J]. J. Alloys Compd., 2017, 692: 713.

[24] Li Y F, Xiao B, Sun L, et al. Phonon optics, thermal expansion tensor, thermodynamic and chemical bonding properties of Al4SiC4 and Al4Si2C5: a first — principles study [J]. RSC Adv., 2016, 6: 43191.

[25] Liao T, Wang J Y, Zhou Y C. Atomistic deformation modes and intrinsic brittleness of Al4SiC4: A first principles investigation [J]. Phys. Rev. B, 2006, 74:174112 .

[26] Sun L, Gao Y M, Li Y F, et al. Structural, bonding, anisotropic mechanical and thermal properties of Al4SiC4 and Al4Si2C5 by first principles investiga-tions [J]. J. Asian Ceram. Soc., 2016, 4: 289.

[27] Forster S. Novel wide bandgap semiconductor material based on ternary carbides — An investigation into Al4SiC4 [D]. Swansea: University of Swansea, 2019.

[28] Pedesseau L, Even J, Modreanu M, et al. Al4SiC4 wurtzite crystal: Structural, optoelectronic, elastic, and piezoelectric properties [J]. APL Mater., 2015, 3: 121101.

[29] Clark S J, Segall M D, Pickard C J, et al., First principles methods using CASTEP [J]. Z. Kristallogr.Cryst. Mater., 2005, 220: 567.

[30] Perdew J P, Burke K, Ernzerhof M. Generalized gradient approximation made simple [J]. Phys. Rev. Lett., 1996, 77: 3865.

[31] Gao J, Liu Q J, Jiang C L, et al. Criteria of mechanical stability of seven crystal systems and its application: Taking silica as an example [J]. Chinese Journal of High Pressure Physics, 2022, 36: 051101

[32] Hill R. The elastic behaviour of a crystalline aggregate [J]. Proc. Phys. Soc. A, 1952, 65: 349.

[33] Pugh S F. XCII. Relations between the elastic moduli and the plastic properties of polycrystalline pure metals [J]. Philos. Mag., 1954, 45: 823.

[34] Fox M. Optical properties of solids [M]. Beijing: Science Press, 2009.